Journal of Applied Electrochemistry (2024) 54:1637–1645
https://doi.org/10.1007/s10800-023-02055-y

RESEARCH ARTICLE

Electrochemical sensing of phenolic pollutant catechol on $LaNiO_3$ perovskite nanostructure platform

Kaveri Krishnamoorthy[1,2] · Narmatha Sivaraman[1,2] · Velayutham Sudha[1,2] · Sakkarapalayam Murugesan Senthil Kumar[1,2] · Rangasamy Thangamuthu[1,2]

Received: 11 September 2023 / Accepted: 28 December 2023 / Published online: 5 February 2024

Abstract

Facile synthesis of perovskite materials for the electrochemical sensing applications are remains challenging. In the current work, a simplified electrochemical sensor system based on an electrode modifier containing $LaNiO_3$ was developed to detect catechol (CC). The surface micrograph of $LaNiO_3$ was examined using X-ray diffraction pattern (XRD), X-ray photoelectron spectroscopy (XPS), and High-resolution transmission electron microscopy (HRTEM). Besides, the $LaNiO_3$ reveals a remarkable electrooxidation response for the detection of catechol by cyclic voltammetry (CV) and amperometry techniques. The suggested sensor platform shows a broad linear range for catechol detection from 5 µM to 2000 µM with LOD and sensitivity of 0.6 µM and 54 µA cm^{-2} mM^{-1}, respectively, under optimised conditions. Furthermore, $LaNiO_3$ altered GCE was fruitfully implemented for the quantification of catechol in tap water sample.

Graphical Abstract

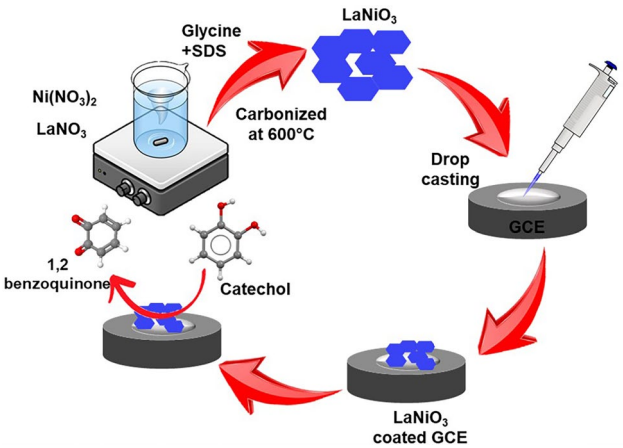

Keywords Electrochemical sensor · Catechol · Cyclic voltammetry · Perovskite material · Inner-transition metal

1 Introduction

Catechol (CC, 1, 2 dihydroxybenzene) is a significant phenolic compound. It is a toxic pollutant to livestock and the environment [1]. Meanwhile, synthetic phenolic compounds are also toxic and constitute pollutants in soil, water and food. Therefore, sensing of phenolic compounds is essential for humans and the environment [2]. Catechol is widely

✉ Rangasamy Thangamuthu
thangamuthu@cecri.res.in; thangamuthu_r@yahoo.co.uk

1 Electroorganic and Materials Electrochemistry (EME) Division, CSIR-Central Electrochemical Research Institute (CSIR-CECRI), Karaikudi, Tamil Nadu 630 003, India

2 Academy of Scientific and Innovative Research (AcSIR), Ghaziabad 201 002, India

used in the manufacture of rubber as a curing agent, skin anti-septic, antioxidant, fungicide, additives in electroplating, photographs, dyes, cosmetics, and many others [3]. It has been reported that catechol affects human health such as upper respiratory tract irritation, high blood pressure, and kidney damage due to its high toxicity and harmful effects on the environment and human health [4]. For the above reason, the determination of catechol is important in the field of environmental monitoring and industrial processes.

Numerous methods are available to determine catechol such as spectroscopic [5], chromatographic [6], chemiluminescence [7], and fluorescence [8]. The above-mentioned methods are feasible but complicated, time-consuming and costly which has limited further commercial application. In comparison to the above method, the electrochemical sensor is the best tool for detecting catechol using modified electrodes [9]. Moreover, the electrooxidation of catechol on bare glassy carbon electrode (GCE) is very poor due to its sluggish electron transfer. Instead of that, modification with nanomaterials has attained higher catalytic activity with lower oxidation potential. Previously, different types of modified electrodes were used to detect catechol like MWCNTs/SPCE [10], Tyr-AuNPs-DHP/GCE [11], AuNPs/Fe_3O_4-APTEs-GO/GCE [12], Au/$Ni(OH)_2$/rGO/GCE [13], AuNPs/ZnO-Al_2O_3/GCE [14], and NiAl-layered/LDHs/GCE [15].

In recent years, interests have focused on nanostructured materials, particularly perovskites attained extensive use in analytical chemistry including solar cells, catalysis, biological sensors, optics, and electronics etc. More interestingly, perovskite material with ABO_3 type metal oxide possesses higher electronic and ionic conductivity with enhanced catalytic activity, chemical and thermal stability by employing variation in oxygen content [16]. Specifically, $LaNiO_3$ is an excellent material that exhibits fascinating chemical and physical characteristics and can be applied as an electrochemical sensing platform to enhance catalytic performance with higher sensitivity [17]. $LaNiO_3$ is a well-known conducting mixed oxide material at room temperature without the use of conducting carbon additive which influences the activity [18]. There are many methods to synthesize $LaNiO_3$ such as sol–gel, hydrothermal, and microwave techniques with diverse nanostructures such as homogeneous and anisotropic morphology, higher conductivity with abundant surface area. Compared with other methods, the simple precipitation method is very effective, low cost, and less time-consuming. Therefore, $LaNiO_3$ is prepared by a simple precipitation method and applied for the electrochemical sensing of catechol [17, 19, 20].

In the present work, we developed $LaNiO_3$ based sensor platform for the sensing of catechol by cyclic voltammetry and amperometry techniques. Synthesized catalyst has been characterized for material purity, elemental composition and morphological studies by XRD, XPS, and HRTEM. The as-synthesized material was used as an electrocatalyst for the detection of phenolic pollutant, catechol. Tap water provided an actual sample to demonstrate the practical application of the $LaNiO_3$ modified electrode.

2 Experimental methods

2.1 Materials

Lanthanum nitrate, nickel nitrate sodium hydroxide, NaH_2PO_4, Na_2HPO_4, sodium dodecyl sulfate (SDS), dimethyl formamide (DMF), hydroxylamine, sodium nitrite ($NaNO_2$), sodium nitrate ($NaNO_3$), and sodium sulphite (Na_2SO_3) were sourced from Sigma-Aldrich. Catechol, dopamine and uric acid were obtained from Sigma Aldrich. All chemicals have been used without additional purification. A double distillation of deionized water from the Milli-Q system was used for the preparation of all solutions.

2.2 Synthesis of $LaNiO_3$

$LaNiO_3$ nanoparticle was synthesized by a simple precipitation method. A stoichiometric amount of lanthanum nitrate (0.01 M) and nickel nitrate (0.01 M) were dissolved in 500 mL distilled water at constant stirring. Then, 0.05 M of glycine was added dropwise into the stirred solution at 100 °C. 0.01 M SDS was injected drop by drop into the hot solution and kept for 12 h at constant stirring. After 12 h, the mixture color was transferred to a dark green precipitate. The precipitate was treated to cool down to room temperature and washed many times with ethanol and water followed by dried in an oven at 85 °C for 12 h and calcinated at 600 °C for 5 h with a heating rate of 5 °C per minute. The final black color material was used as an electrocatalyst for the detection of catechol.

2.3 Fabrication of $LaNiO_3$ modified electrode

Primarily, mirror-like surface of GCE was cleaned using 0.05 micron alumina powder on a polishing pad. Further, the electrode was washed with water and sonicated to remove alumina particles. The catalyst slurry was prepared by mixing 5 mg of $LaNiO_3$ in 1 mL of DMF solvent and sonicated for 30 min. After sonication, 3 µL catalyst was dropped over precleaned GCE and allowed to dry. Finally, the obtained $LaNiO_3$ modified GCE was used to detect CC in the present study as shown in Scheme 1.

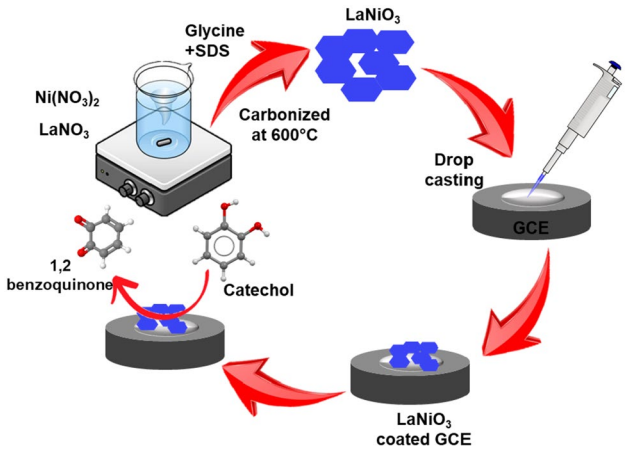

Scheme 1 Stepwise fabrication of $LaNiO_3$ modified GC electrode for catechol sensing

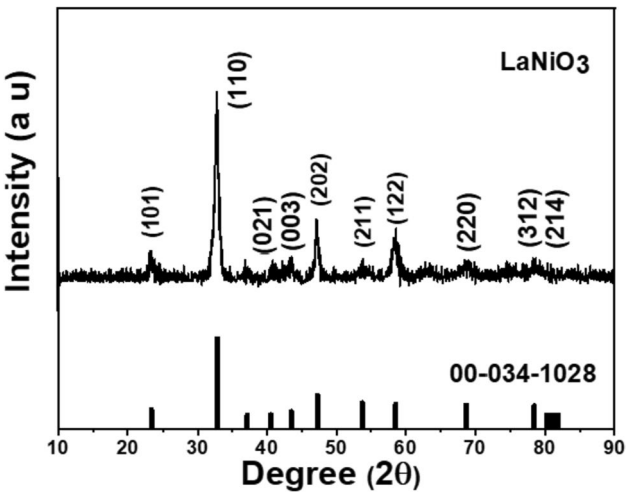

Fig. 1 XRD pattern of as-prepared $LaNiO_3$

3 Result and discussion

3.1 Physical characterization of $LaNiO_3$

The XRD pattern of $LaNiO_3$ is shown in Fig. 1. $LaNiO_3$ displays the perovskite phase with crystal planes of (101), (110), (021), (003), (202), (211), (122), (220), (312), and (214) corresponding 2θ values at 23°, 32°, 40°, 41°, 47°, 53°, 58°, 68°, 78°, and 79°, respectively. The distinctive diffraction peaks of $LaNiO_3$ exactly match with the ICDD number 00-034-1028 and a hexagonal structure [21]. We can conclude from the XRD results that $LaNiO_3$ exists in a well-crystalline, hexagonal form with no impurities being visible. As a result, the synthesized $LaNiO_3$ is of a high purity, proving that the synthesis approach can be applied for large-scale preparation.

HRTEM is mainly used for the detection of higher-resolution surface morphology and SAED pattern. Figure 2 shows the surface morphology and SAED pattern of $LaNiO_3$. Several magnifications such as 200 nm, 100 nm, and 50 nm are shown in Fig. 2A, B, and C, respectively. The selected area electron diffraction pattern (SAED) of $LaNiO_3$ is shown in Fig. 2D. Figure 2D confirms that our synthesized $LaNiO_3$ was perfectly crystalline in nature. The d spacing values were estimated from the SAED pattern and the value are well matched with the XRD results. Based on the HRTEM micrographs, the synthesized $LaNiO_3$ had well-crystalline nature and nanostructured material.

The XPS survey spectrum displays multiple peaks that are related to Ni 2p, La 3d, and O 1s which is shown in Fig. 3A. Figure 3B shows peaks for La $3d_{5/2}$ and La $3d_{3/2}$ at 836 eV and 854 eV, respectively, which is comparable with the results of lanthanum in a La (III) oxidation state that have been reported [22]. The higher-resolution XPS studies of Ni $2p_{1/2}$ and Ni $2p_{3/2}$ peaks and corresponding satellite peaks of $LaNiO_3$ are shown in Fig. 3C. Figure 3C clearly indicates that Ni $2p_{1/2}$ and Ni $2p_{3/2}$ peaks were exhibited at 872 eV and 854 eV, respectively [23]. As exhibited in Fig. 3D, the binding energy (BE) of O 1s peaks observed at 529 eV and 531 eV [24, 25].

3.2 Electrochemical characterization studies of $LaNiO_3$ modified electrode

3.2.1 Cyclic voltammetry

Synthesized $LaNiO_3$ was utilized for the electrochemical oxidation of catechol. $LaNiO_3$ altered GCE was employed for the electrochemical oxidation of catechol in 0.1 M PBS using CV technique (pH = 7). Figure 4 shows CVs of bare GCE and $LaNiO_3$/GCE in the presence and absence of catechol. Curve 'a' and 'b' indicate that bare GCE and $LaNiO_3$ altered GCE in the absence of catechol. There was no current response in pure PBS electrolyte. Curve 'c' and 'd' indicate the bare GCE and modified GCE with the existence of 1 mM catechol at 10 mV s^{-1} scan rate. However, compared to bare GCE, $LaNiO_3$ modified GCE shows higher current density response towards the sensing of catechol. The observed higher current response of $LaNiO_3$/GCE to the electrooxidation of catechol is attributed to the electrocatalytic activity of $LaNiO_3$.

The pH effect on electrochemical sensing of catechol at $LaNiO_3$/GCE was investigated using CV studies with 1 mM catechol at a sweeping rate of 10 mV s^{-1}. Figure 5A exhibits CVs of catechol at different pH such as 6.0, 6.5, 7.0, 7.5, and 8.0. Figure 5B illustrates the increment in peak current when the pH increases from pH 6 to pH 7, then it starts

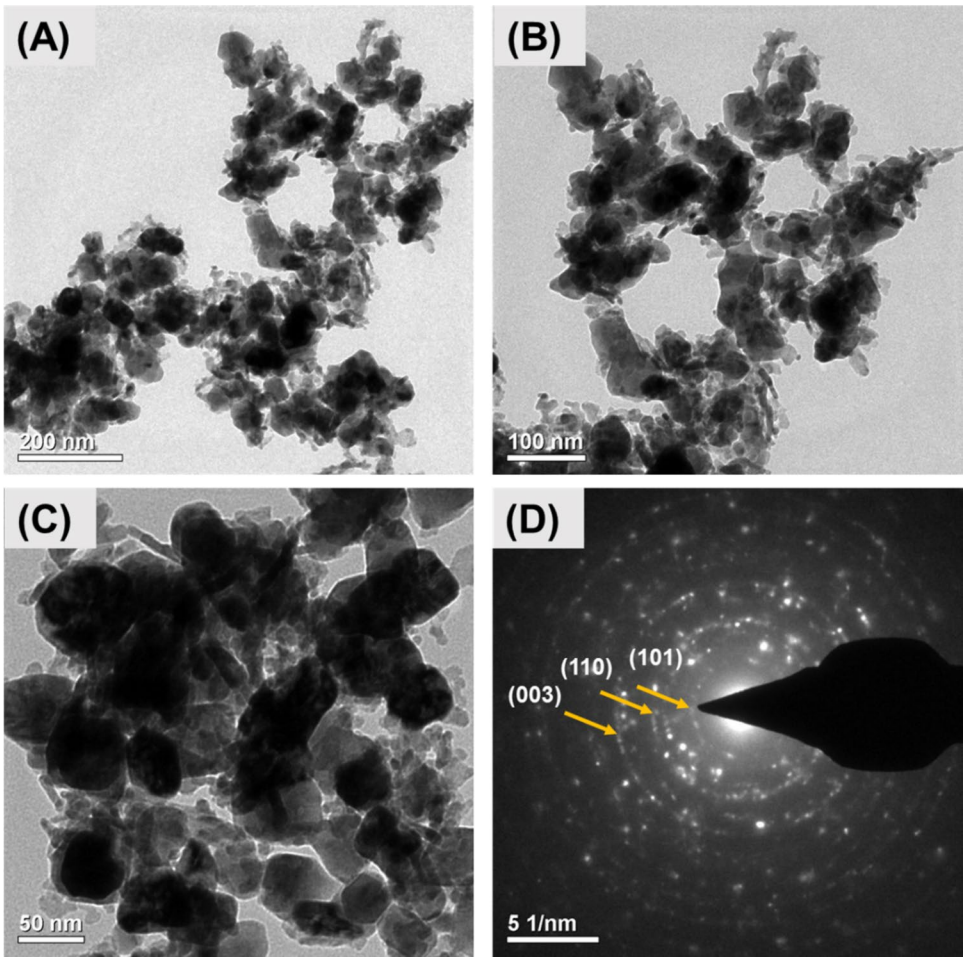

Fig. 2 **A** HRTEM of $LaNiO_3$ with 200 nm scale magnification size; **B**, **C** Corresponds to 100 nm and 50 nm magnification images and **D** SAED pattern of $LaNiO_3$

to diminish when pH increases further. Therefore, the optimized PBS (pH = 7) was chosen for further electrochemical studies. From the results, the probable reaction mechanism of catechol at $LaNiO_3$ altered GCE is displayed in Fig. 5C.

Electrocatalytic behavior of $LaNiO_3$/GCE at various concentrations of catechol has been investigated using CV in 0.1 M PBS in pH = 7 (10 mV s^{-1}). The CV responses for electrocatalytic determination of catechol at $LaNiO_3$/GCE upon each addition of catechol are disclosed in Fig. 6A. Anodic peak current augmented with the increment of catechol concentration from 0.05 to 10 mM. Figure 6B displayed that anodic peak current varies linearly with catechol concentration in the range from 0.05 to 7 mM. From the calibration curves in Fig. 6B, the obtained sensitivity value is 95 µA cm^{-2} mM^{-1} with its corresponding linear regression equation $I_{p.a.} = 95x + 39 \times (C)$ mM ($R^2 = 0.989$).

To understand kinetics, CVs of $LaNiO_3$/GCE in 0.1 M PBS with the existence of 1 mM catechol were recorded at various scan rates. Figure 6C shows the oxidative peak current amplified steadily with an increment of scan rate starting from 10 to 150 mV s^{-1} and further positive shift was observed in the peak potential. The peak current was correlated with scan rate as displayed in Fig. 6D ($R^2 = 0.992$). Linear response was observed for the current density with square root of scan rate, which signifies the electron transfer process was under mass-transfer control.

3.2.2 Amperometric study

Amperometric measurement was carried out at an optimized applied potential of 0.3 V using $LaNiO_3$/GCE by successive addition of different concentrations of catechol in 0.1 M PBS (pH 7). Figure 7A exhibits the response of modified electrode at different concentrations of catechol from 5 µM to 8 mM. Figure 7B displays the current response of $LaNiO_3$ for the successive addition of catechol. By increasing the catechol concentration from 5 to 2000 µM, current response increased gradually. From the calibration plot in Fig. 7B, sensitivity and detection limit (LOD) were calculated as 54 µA cm^{-2} mM^{-1} and 0.6 µM, respectively, with $I_{p.a.} = 54x + 4.9 \times (C)$ mM linear regression equation ($R^2 = 0.994$). A comparison of analytical parameters of our proposed sensor with other modified electrodes for catechol sensing is displayed in Table 1. It can be seen that our proposed

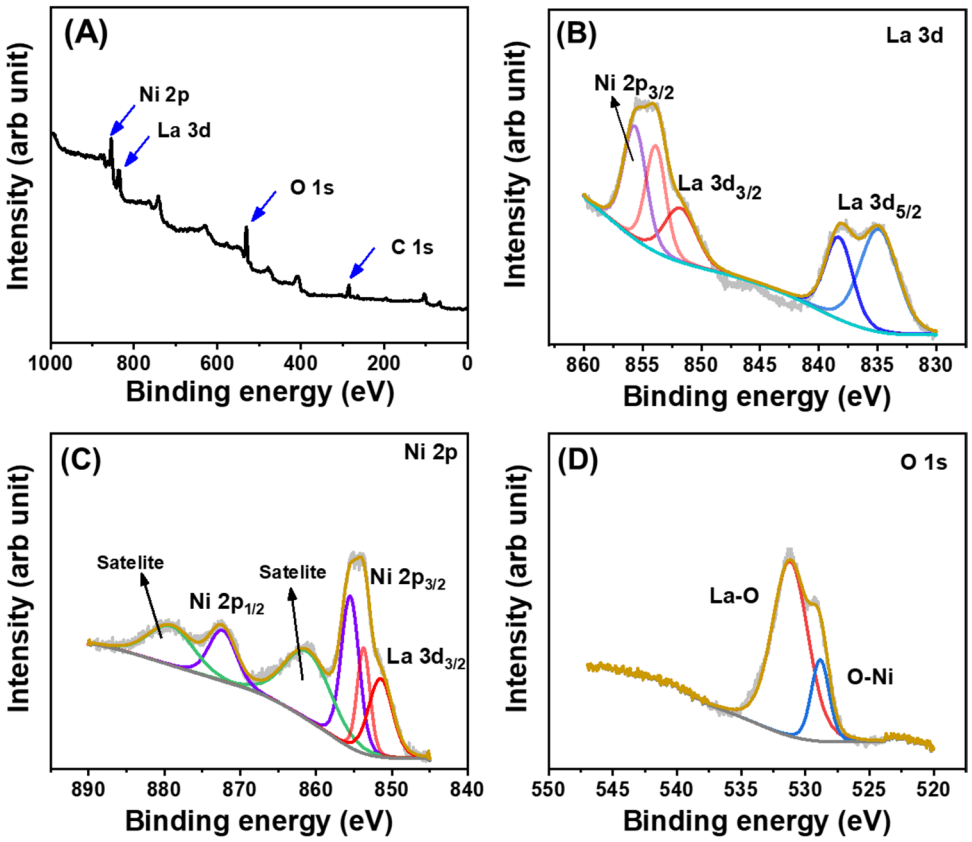

Fig. 3 XPS spectra (**A**) Survey scan of $LaNiO_3$; **B** La 3d; **C** Ni 2p and **D** O 1s spectrum

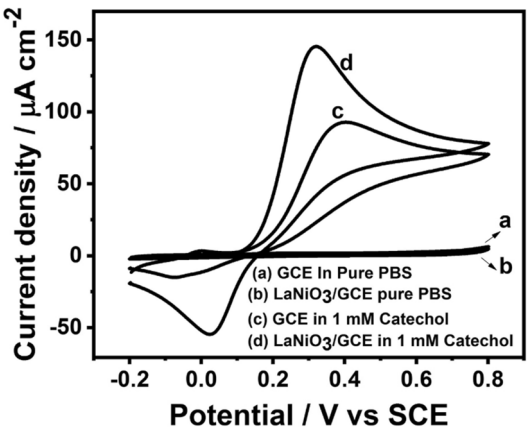

Fig. 4 CV of bare GCE; $LaNiO_3$/GCE in pure 0.1 M PBS with pH = 7; bare GCE and $LaNiO_3$ /GCE with 1 mM catechol. Sweeping rate = 10 mV s^{-1}

electrode shows wide concentration range compared to other electrodes.

Selectivity of the proposed sensor for the sensing of catechol was further assessed by amperometric analysis at 0.3 V (0.1 M PBS). Figure 8A depicts the amperometric response of $LaNiO_3$/GCE for the determination of catechol in the existence of common interferents with 50-fold higher concentration of resorcinol, hydroquinone, ammonia nitrate, sodium nitrite, sodium bromate, potassium chloride, calcium carbonate, sodium sulfite, ascorbic acid, glucose, and urea. The obtained amperometric response clearly indicates that our proposed sensor could selectively sense the catechol and no significant current change was observed for the addition of other interferents. Figure 8B depicts the corresponding bar diagram of the interference which are included along with catechol. The above result clearly explains that our proposed sensor has high selectivity to detect catechol even in the presence of a high concentration of common interferent exist in solution.

3.2.3 Practical application

Real time application of $LaNiO_3$/GCE sensor examined with the utilization of real sample (tap water). The tap water was collected from our institute (Karaikudi, Tamil Nadu, India). To perform a real sample analysis of catechol, a known amount (10 mM) of catechol was spiked in the water sample. The amperometric measurements were carried out by adding different known concentrations of catechol via the standard spiking method. A known quantity of standard catechol solution (25 and 50 μM) was spiked into the 0.1 M PBS as illustrated in Fig. 9A. The corresponding linear calibration plot of different addition of catechol into the real sample is shown in Fig. 9B. The obtained data validate that our sensor

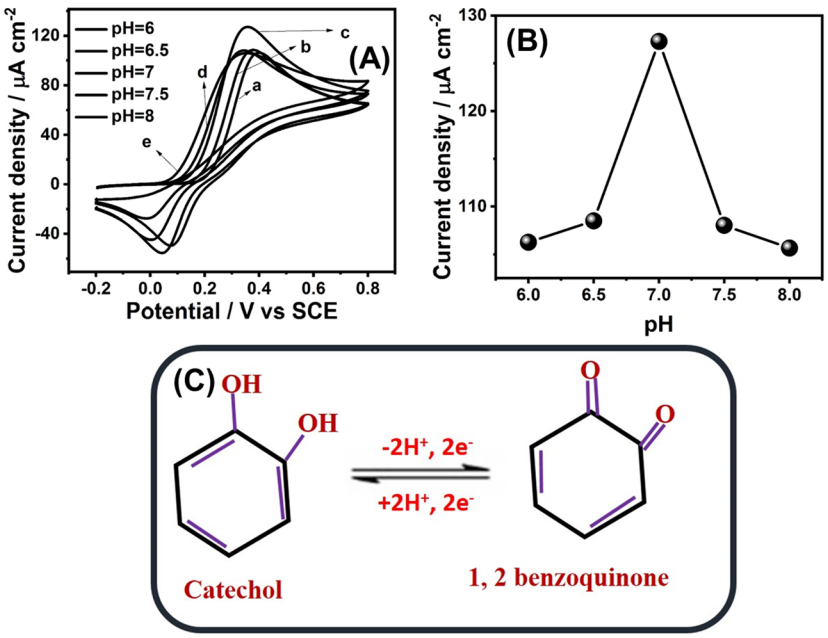

Fig. 5 **A** CVs of $LaNiO_3$/GCE in 1 mM catechol under various pH (6.0, 6.5, 7.0, 7.5, and 8.0) in 0.1 M PBS (10 mV s^{-1}); **B** Current density *ν*s pH curve for the electrochemical sensing of catechol at $LaNiO_3$/GCE and **C** The electrochemical oxidation mechanism of catechol on $LaNiO_3$/GCE

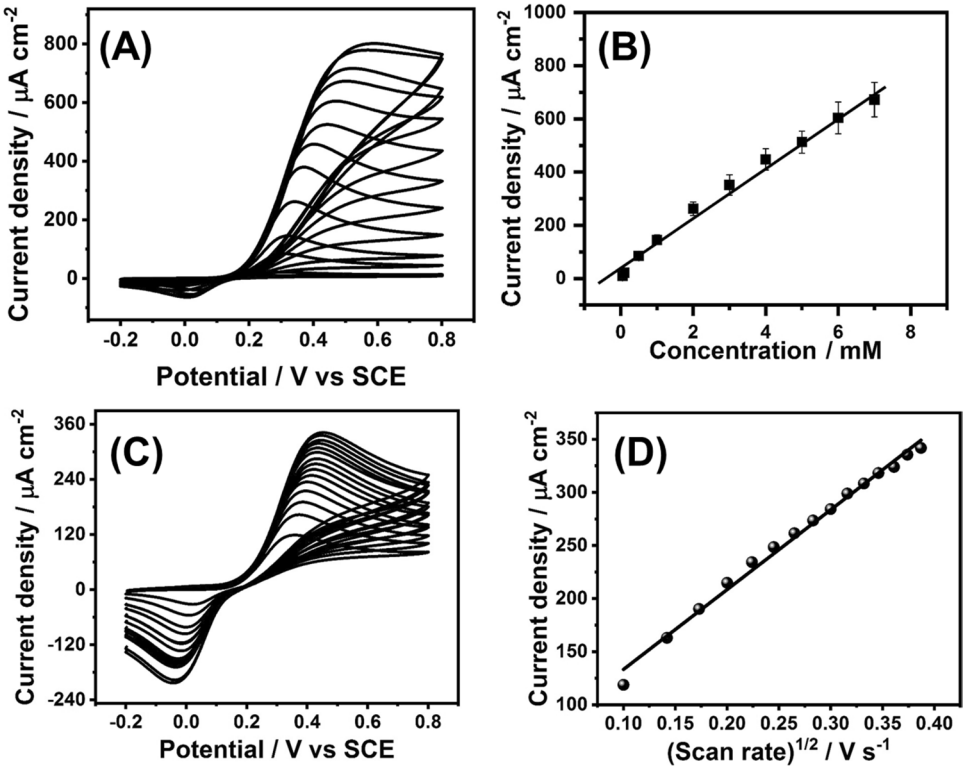

Fig. 6 **A** Cyclic voltammograms of different concentrations of catechol at $LaNiO_3$/GCE. Concentration of catechol 0.05–10 mM. Scan rate = 10 mV s^{-1}. **B** Calibration plot. **C** Cyclic voltammograms of 1 mM catechol at $LaNiO_3$/GCE with an increment of scanning rate starts from 10 to 150 mV s^{-1} and **D** Dependence of J *ν*s (scan rate)$^{1/2}$

could be effective for catechol detection in water samples with good RSD values.

3.2.4 Stability and reproducibility

Stability of the $LaNiO_3$/GCE was determined with 1 mM of catechol by continuously recording 100 cyclic voltammograms as shown in Fig. 10. Stable current was observed with less than 5% relative standard deviation (RSD) in their current values. The CV results reveal that the $LaNiO_3$/GCE modified electrodes exhibits appreciable stability. Reproducibility of the fabricated electrode was carried

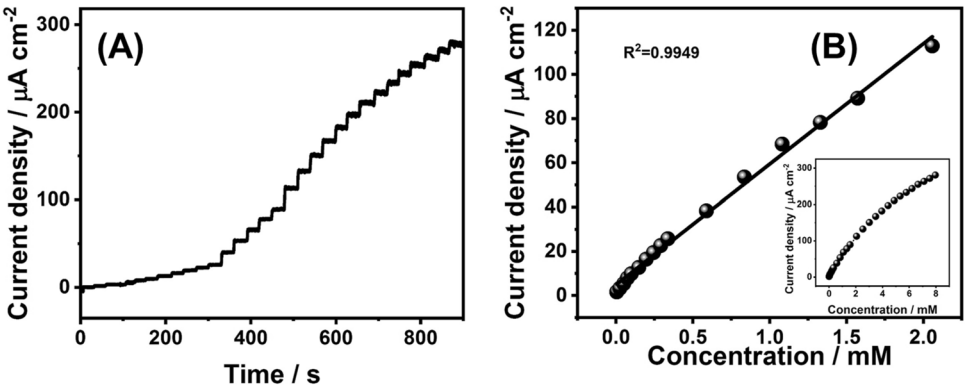

Fig. 7 **A** Amperometric response of $LaNiO_3$/GCE at different concentrations of catechol from 5 µM to 8 mM and **B** Corresponding linear calibration curve for the concentration 5 µM to 2 mM. Applied potential = 0.3 V. Insert of Figure B shows a calibration curve of the entire concentration range (5 µM to 8 mM)

Table 1 Comparison of analytical parameters for catechol sensing using different modified electrodes

Modified electrodes	Method	Detection limit (LOD) (µM)	Linear range (µM)	Sensitivity (µA mM^{-1} cm^{-2})	References
EGr-TPy/GCE	DPV	0.303	1–100	3.22	[4]
CD-f-CSA-PEDOT: PSS	CV	0.0095	0.05–200	NR	[26]
H-NiAl/LDHs/GCE	i–t	0.02	0.01–400	418.3	[15]
Au/$Ni(OH)_2$/rGO/GCE	DPV	0.13	0.4–33.8	NR	[13]
Fe/APTMs/GO	i–t	1.1	3–112	1184.3	[27]
AuNPs/CS@N,S co-doped MWCNTS	i–t	0.2	1–5000	0.90	[9]
Po-DG6-MCPE	DPV	0.09	20–160 µM	NR	[28]
Co_3O_4/MWCNTs	DPV	8.5	10–700	NR	[29]
$LaNiO_3$/GCE	i–t	0.6	5–2000	54	This work

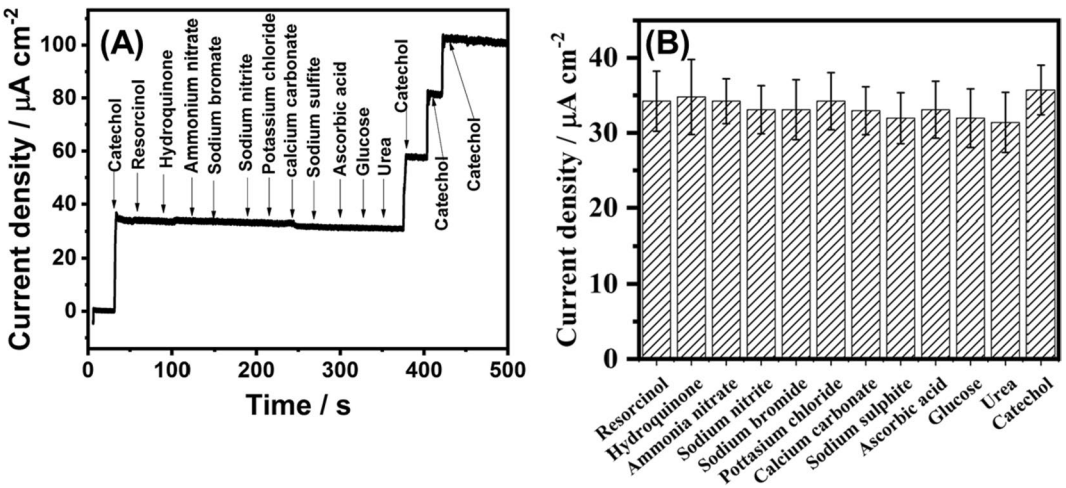

Fig. 8 **A** Amperometric responses of $LaNiO_3$/GCE modified electrode to the addition of 100 µL stock solution addition of catechol and addition of 50-fold high concentration of resorcinol, hydroquinone, ammonia nitrate, sodium nitrite, sodium bromate, potassium chloride, calcium carbonate, sodium sulfite, ascorbic acid, glucose, and urea at 0.3 V. **B** Corresponding bar diagram of the interference study

out using 5 different modified electrodes with an RSD of less than 4.5%, which confirms that $LaNiO_3$ modified GCEs have appreciable fabrication reproducibility. Hence, $LaNiO_3$/GCE can be employed for practical applications.

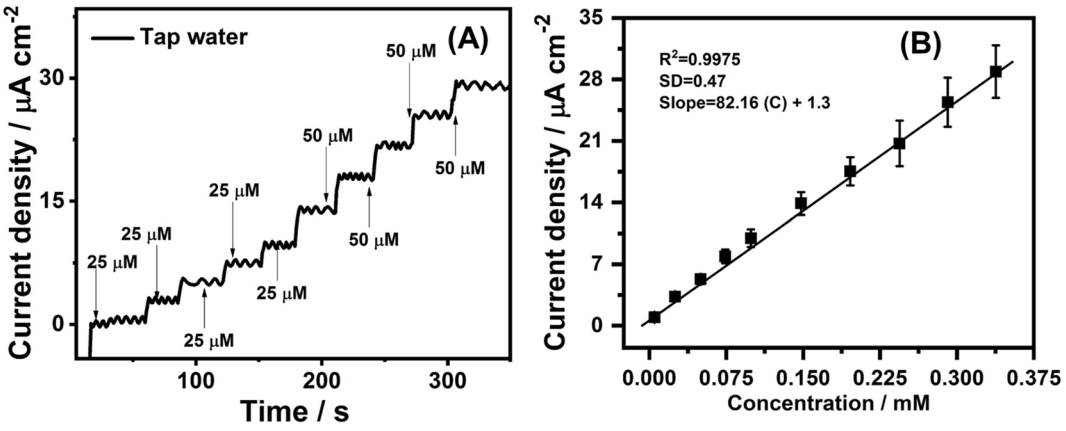

Fig. 9 **A** Amperometric response of catechol with various additions in tap water sample and **B** Corresponding linear calibration plot

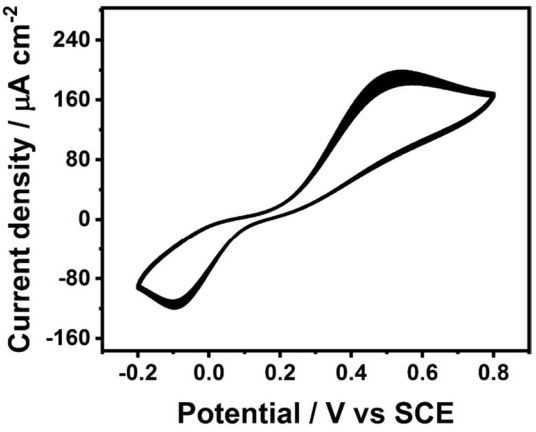

Fig. 10 Electrode stability test recorded in 0.1 M catechol (0.1 M PBS) with 10 mV s^{-1} scan rate for continuous cycles of 100

4 Conclusion

In summary, we have explored a highly sensitive catechol sensor by employing a $LaNiO_3$ perovskite nanostructure-modified electrode. The XPS spectra revealed the various oxidation states of the as-prepared materials. The proposed sensor exhibited enhanced analytical features towards the determination of catechol with higher sensitivity (54 μA cm^{-2} mM^{-1}), lower detection limit (0.6 μM), eminent selectivity, wide linear range (5 to 2000 μM), and stability. Moreover, the estimation of catechol in tap water encourages the chance for real time application towards the proposed $LaNiO_3$ as a modifier. Hence, it is believed that the $LaNiO_3$ nanocomposite-modified electrode can be considered as a promising material for sensor application.

Acknowledgements K. Krishnamoorthy would like to thank CSIR-UGC, New Delhi for financial support. We wish to acknowledge the Central Instrumentation Facility (CIF), CSIR-CECRI, Karaikudi for characterization studies. Manuscript number: CECRI/PESVC/Pubs/2023-062.

Author contributions KK-writing—original draft, and investigation, SN-writing—review and editing, VS-writing—review and editing, SMSK-investigation and formal analysis, RT-supervision, conceptualization and review and editing.

Funding K. Krishnamoorthy would like to thank CSIR-UGC, New Delhi for financial support.

Data availability Data will be available on request.

Declarations

Competing interest The authors declared that there is no conflict of interest.

References

1. Liang Y, Li J, Zhao Y (2017) Poly (sulfosalicylic acid)/ multi-walled Carbon Nanotube Modified Electrode for the Electrochemical Detection of Catechol. Int J Electrochem Sci 12:9512–9522. https://doi.org/10.20964/2017.10.20
2. Dorraji PS, Jalali F (2015) A Nanocomposite of Poly (melamine) and Electrochemically Reduced Graphene Oxide Decorated with Cu Nanoparticles: Application to Simultaneous Determination of Hydroquinone and Catechol. J Electrochem Soc 162:237–244. https://doi.org/10.1149/2.0951509jes
3. Matos F, De, Deon M, Nicolodi S et al (2018) Electrochimica acta magnetic silica / titania xerogel applied as electrochemical biosensor for catechol and catecholamines. Electrochim Acta 264:319–328. https://doi.org/10.1016/j.electacta.2018.01.127
4. Coros M, Pog F, Lidia M (2017) Graphene-porphyrin composite synthesis through graphite exfoliation: the electrochemical sensing of catechol. Sens Actuators B. https://doi.org/10.1016/j.snb.2017.09.205
5. Smith SJ, Noble ÆCJ, Palmer ÆRC et al (2008) Structural and spectroscopic studies of a model for catechol oxidase. J Biol Inorg Chem 13:499–510. https://doi.org/10.1007/s00775-007-0334-7
6. Lan L, Wu S, Yu S et al (2019) Fast and direct determination of catechol-3, 6-bis (methyleiminodiacetic acid) prototype in beagle

dog plasma using liquid chromatography tandem mass spectrometry : a simplified and high throughput in-vivo method for the metal chelator. J Chromatogr A 1596:84–95. https://doi.org/10.1016/j.chroma.2019.03.002
7. Yang D, He Y, Sui Y, Chen F (2017) Determination of catechol in water based on gold nanoclusters-catalyzed chemiluminescence. J Lumin 187:186–192. https://doi.org/10.1016/j.jlumin.2017.02.067
8. Han S, Liu B, Liu Y, Fan Z (2016) Silver nanoparticle induced chemiluminescence of the hexacyanoferrate-fluorescein system, and its application to the determination of catechol. Microchim Acta 183:917–921. https://doi.org/10.1007/s00604-015-1704-4
9. Rao H, Liu Y, Zhong J et al (2017) Gold Nanoparticle/Chitosan@N,S co-doped multiwalled carbon nanotubes sensor: fabrication, characterization, and electrochemical detection of catechol and nitrite. ACS Sustain Chem Eng 5:10926–10939. https://doi.org/10.1021/acssuschemeng.7b02840
10. Rao MM, Settu R, Chen S, Alagarsamy P (2018) Electrochemical Determination of Catechol Using Functionalized Multiwalled Carbon Nanotubes modified Screen Printed Carbon Electrode. Int J Electrochem 13:6126–6134. https://doi.org/10.20964/2018.06.121
11. Vicentini FC, Garcia LLC, Figueiredo-filho LCS et al (2015) A biosensor based on gold nanoparticles, dihexadecylphosphate, and tyrosinase for the determination of catechol in natural water. Enzyme Microbial Technol. https://doi.org/10.1016/j.enzmictec.2015.12.004
12. Erogul S, Bas SZ, Ozmen M, Yildiz S (2015) A new electrochemical sensor based on Fe_3O_4 functionalized graphene oxide-gold nanoparticle composite film for simultaneous determination of catechol and hydroquinone. Electrochim Acta 186:302–313. https://doi.org/10.1016/j.electacta.2015.10.174
13. Wang H, Qu J, Wang Y et al (2017) Analytical methods nanocomposites supported on reduced graphene. Anal Methods 9:338–344. https://doi.org/10.1039/c6ay02814d
14. Nazari M, Kashanian S, Moradipour P, Maleki N (2018) A novel fabrication of sensor using ZnO-Al2O3 ceramic nanofibers to simultaneously detect catechol and hydroquinone. J Electroanal Chem. https://doi.org/10.1016/j.jelechem.2018.01.058
15. Shen M, Zhang Z, Ding Y (2016) Synthesizing NiAl-layered double hydroxide microspheres with hierarchical structure and electrochemical detection of hydroquinone and catechol. Microchem J 124:209–214. https://doi.org/10.1016/j.microc.2015.08.011
16. George KJ, Halali VV, Sanjayan CG et al (2020) Perovskite nanomaterials as optical and electrochemical sensors. Inorg Chem Front 7:2702–2725. https://doi.org/10.1039/D0QI00306A
17. Wang B, Gu S, Ding Y et al (2013) A novel route to prepare $LaNiO_3$ perovskite-type oxide nanofibers by electrospinning for glucose and hydrogen peroxide sensing. Analyst 138:362–367. https://doi.org/10.1039/C2AN35989H
18. Petrie JR, Cooper VR, Freeland JW et al (2016) Enhanced bifunctional oxygen catalysis in strained $LaNiO_3$ Perovskites. J Am Chem Soc 138:2488–2491. https://doi.org/10.1021/jacs.5b11713
19. Forslund RP, Mefford JT, Hardin WG et al (2016) Nanostructured $LaNiO_3$ perovskite electrocatalyst for enhanced urea oxidation. ACS Catal 6:5044–5051. https://doi.org/10.1021/acscatal.6b00487
20. Mcbean CL, Liu H, Sco ME et al (2017) Generalizable, electroless, template-assisted synthesis and electrocatalytic mechanistic understanding of perovskite $LaNiO_3$ nanorods as viable, supportless oxygen evolution reaction catalysts in alkaline media. ACS Appl Mater Interfaces. https://doi.org/10.1021/acsami.7b06855
21. Mao M, Xu J, Li L et al (2019) High performance hydrogen production of MoS_2-modified perovskite $LaNiO_3$ under visible light. Ionics 25:4533–4546. https://doi.org/10.1007/s11581-019-03210-2
22. Sales HBE, Inocêncio CVM, Varga E et al (2017) CO_2 reforming of methane over supported $LaNiO_3$ perovskite-type oxides. Appl Catal B. https://doi.org/10.1016/j.apcatb.2017.09.022
23. Xu J, Sun C, Wang Z et al (2018) Perovskite oxide $LaNiO_3$ nanoparticles for boosting H_2 evolution over commercial CdS with visible light. Chem Eur J 1:18512–18517. https://doi.org/10.1002/chem.201802920
24. Sun M, Zhang Q, Chen Q et al (2022) Coupling $LaNiO_3$ Nanorods with FeOOH Nanosheets for Oxygen Evolution Reaction. Catalysts 12:594
25. Qiu Y, Gao R, Yang W et al (2020) Understanding the enhancement mechanism of a-site-deficient $LaxNiO_3$ as an oxygen redox catalyst. Chem Mater 32:1864–1875. https://doi.org/10.1021/acs.chemmater.9b04287
26. Qian Y, Ma C, Zhang S et al (2017) High performance electrochemical electrode based on polymeric composite film for sensing of dopamine and catechol. Sens Actuators B Chem. https://doi.org/10.1016/j.snb.2017.08.174
27. Elancheziyan M, Manoj D, Saravanakumar D (2017) Amperometric sensing of catechol using a glassy carbon electrode modified with ferrocene covalently immobilized on graphene oxide. Microchimica Acta 184:2925–2932. https://doi.org/10.1007/s00604-017-2312-2
28. Chetankumar K, Kumara Swamy BE, Sharma SC, Hariprasad SA (2021) An efficient electrochemical sensing of hazardous catechol and hydroquinone at direct green 6 decorated carbon paste electrode. Sci Rep 11:15064. https://doi.org/10.1038/s41598-021-93749-w
29. Song Y, Zhao M, Wang X et al (2019) Simultaneous electrochemical determination of catechol and hydroquinone in seawater using Co_3O_4/MWCNTs/GCE. Mater Chem Phys 234:217–223. https://doi.org/10.1016/j.matchemphys.2019.05.071